JACS
JOURNAL OF THE AMERICAN CHEMICAL SOCIETY
Article
pubs.acs.org/JACS

Are Free Radicals Involved in IspH Catalysis? An EPR and Crystallographic Investigation

Weixue Wang,[†] Ke Wang,[‡] Ingrid Span,[⊥] Johann Jauch,[∥] Adelbert Bacher,[⊥] Michael Groll,[⊥] and Eric Oldfield*[,†,‡]

[†]Center for Biophysics and Computational Biology, 607 South Mathews Avenue, and [‡]Department of Chemistry, 600 South Mathews Avenue, University of Illinois at Urbana-Champaign, Urbana, Illinois 61801, United States

[⊥]Center for Integrated Protein Science, Chair of Biochemistry, Chemistry Department, Technische Universität München, Lichtenbergstrasse 4, 85747 Garching, Germany

[∥]Organische Chemie II, Universität des Saarlandes, Postfach 15 11 50, 66041 Saarbrücken, Germany

Supporting Information

ABSTRACT: The [4Fe−4S] protein IspH in the methylerythritol phosphate isoprenoid biosynthesis pathway is an important anti-infective drug target, but its mechanism of action is still the subject of debate. Here, by using electron paramagnetic resonance (EPR) spectroscopy and ^{2}H, ^{17}O, and ^{57}Fe isotopic labeling, we have characterized and assigned two key reaction intermediates in IspH catalysis. The results are consistent with the bioorganometallic mechanism proposed earlier, and the mechanism is proposed to have similarities to that of ferredoxin, thioredoxin reductase, in that one electron is transferred to the $[4Fe-4S]^{2+}$ cluster, which then performs a formal two-electron reduction of its substrate, generating an oxidized high potential iron−sulfur protein (HiPIP)-like intermediate. The two paramagnetic reaction intermediates observed correspond to the two intermediates proposed in the bioorganometallic mechanism: the early π-complex in which the substrate's 3-CH_2OH group has rotated away from the reduced iron−sulfur cluster, and the next, η^3-allyl complex formed after dehydroxylation. No free radical intermediates are observed, and the two paramagnetic intermediates observed do not fit in a Birch reduction-like or ferraoxetane mechanism. Additionally, we show by using EPR spectroscopy and X-ray crystallography that two substrate analogues (**4** and **5**) follow the same reaction mechanism.

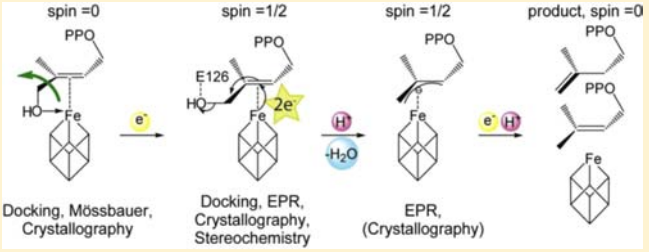

INTRODUCTION

(*E*)-4-Hydroxy-3-methyl-but-2-enyl diphosphate (HMBPP, **1**) reductase (EC 1.17.1.2, IspH, also known as LytB) is the last enzyme in the methylerythritol phosphate isoprenoid biosynthesis pathway.[1] It contains a [4Fe−4S] cluster with a unique fourth iron not coordinated to any cysteine residue,[2−5] and catalyzes the $2H^+/2e^-$ reduction of **1** to isopentenyl diphosphate (**2**) and dimethylallyl diphosphate (**3**) in a ∼5:1 ratio (Scheme 1).[6,7] Since these compounds are key building blocks in isoprenoid biosynthesis, IspH is essential for survival of most bacteria, plants, as well as malaria parasites. However, it is not produced by humans, who use the mevalonate pathway for isoprenoid biosynthesis. IspH is thus of interest as a drug target, and several inhibitors have been reported.[8−12] The catalytic mechanism has, however, been a mystery for many years, and previous studies have proposed several mechanisms including cationic, anionic, radical, and diene intermediates.[2,6,7,13,14]

Scheme 1. Reaction Catalyzed by IspH, and Two Substrate Analogues (4, 5)

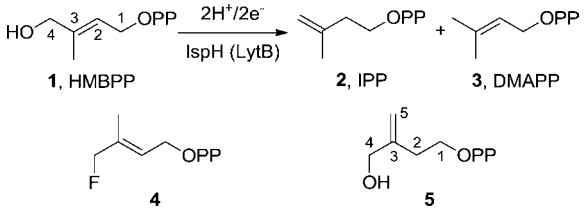

On the basis of computational docking,[15] and an electron paramagnetic resonance (EPR) study of a reaction intermediate trapped by the inactive *Aquifex aeolicus* IspH E126A mutant,[9] we previously proposed a bioorganometallic mechanism of IspH action[9] whose key reaction intermediates are summarized in Scheme 2. In this mechanism, HMBPP (**1**) initially binds to the unique fourth iron of the $[4Fe-4S]^{2+}$ cluster via its terminal 4-OH group, forming Intermediate I, an alkoxide (or alcohol) complex **6**. On reduction, the 3-hydroxymethyl (3-CH_2OH) group rotates away from the iron−sulfur cluster to form Intermediate II, a π-complex **7**, drawn alternatively as the metallacycle **8**. This intermediate then loses an H_2O molecule

Received: April 10, 2012
Published: June 12, 2012

dx.doi.org/10.1021/ja303445z | J. Am. Chem. Soc. 2012, 134, 11225−11234

Scheme 2. Reaction Intermediates Proposed in the Bioorganometallic Mechanism of IspH Catalysis[9]

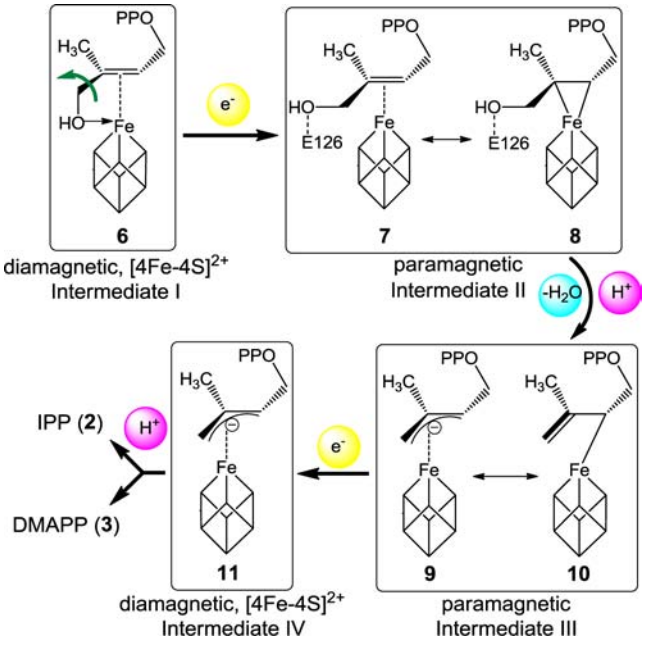

to form Intermediate III, an η^3-allyl anion **9**, which can also be drawn as its resonance form, an η^1-complex **10**, bonded to the unique fourth iron. Following the second e^- and H^+ delivery, the final products **2** and **3** are formed. In this mechanism, direct iron–carbon interactions play an important role in catalysis, and no free radicals are involved. Recently, this bioorganometallic mechanism was challenged on the basis of the results of reactions of IspH with fluoro analogues of **1** (e.g., **4**)[16] as well as an isomer of **1** ("*iso*-HMBPP", **5**).[17] These workers favored a Birch reduction-like mechanism (Scheme 3), and ruled out the bioorganometallic mechanism, a conclusion at odds with a recent stereochemical study.[18]

Scheme 3. Birch Reduction-like Mechanism of IspH Catalysis[16]

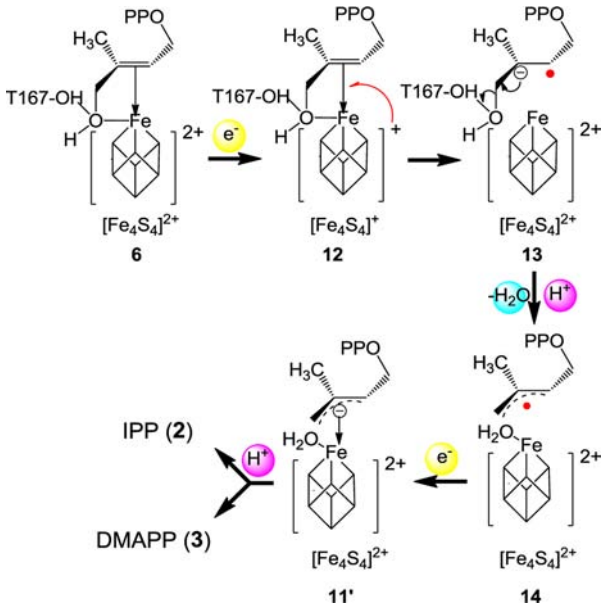

In order to help clarify the mechanism of IspH catalysis, we report here the results of an EPR spectroscopic and X-ray crystallographic investigation that provide new insights into the nature of the reaction intermediates. On the basis of EPR and hyperfine sublevel correlation (HYSCORE) spectroscopy and ^{17}O-labeling, the structure of the reaction intermediate trapped with IspH mutants is assigned to Intermediate II; on the basis of EPR spectroscopy and ^{2}H, ^{17}O, and ^{57}Fe-labeling, a second reaction intermediate trapped with wild-type IspH is assigned to Intermediate III. We also show that [4Fe–4S] clusters coordinated with π-ligands exhibit a novel class of **g** tensors. Taken together, the results show that current as well as previous EPR spectroscopic and X-ray crystallographic data fit the bioorganometallic mechanism (Scheme 2), but not the Birch reduction-like mechanism (Scheme 3), in addition to suggesting similarities between the mechanisms of action of IspH and other proteins that have high potential iron–sulfur protein (HiPIP)-like intermediates.

RESULTS AND DISCUSSION

The Intermediate Trapped with an E126A/E126Q IspH Mutant Is Intermediate II, a Weak π-Complex with a Rotated Substrate 3-CH$_2$OH Group. Previous studies showed that a reaction intermediate can be trapped by adding **1** to an unreactive *A. aeolicus* IspH E126A mutant, and that its EPR spectrum was characterized by a **g** tensor having principal values of [2.124, 1.999, 1.958].[9] With an *Escherichia coli* IspH E126Q mutant, a similar intermediate is obtained, characterized by **g** = [2.132, 2.003, 1.972] (Figure 1A). These **g** tensor values are reminiscent of those seen previously with ethylene and allyl alcohol bound to the α-70Ala mutant of a nitrogenase FeMo cofactor protein (ethylene: **g** = [2.123, 1.978, 1.949];[19] allyl alcohol: **g** = [2.123, 1.998, 1.986][20]), where it was proposed that a metallacycle formed with, on average, only a ~0.01 difference between the IspH and nitrogenase *g*-values. Despite the similar **g** tensor values to those of metallacycles formed in nitrogenase, it has recently been proposed that the key coordination to the [4Fe–4S] cluster is the 4-OH group of **1**; interactions between the C=C of **1** and the [4Fe–4S] cluster not being essential for catalysis.[16,17]

To investigate whether Fe–O4 bonding is present in this intermediate, we prepared [4-^{17}O]-**1** (70% ^{17}O enrichment), and carried out an ^{17}O-hyperfine sublevel correlation (HYSCORE) investigation. HYSCORE spectra of the *E. coli* IspH E126Q mutant incubated with [4-^{17}O]-**1** collected at three different τ-values show the presence of only a very weak ^{17}O hyperfine interaction (~1 MHz, Figure 1B). In other iron–sulfur proteins (e.g., aconitase), Fe–O bonding usually results in ~8–15 MHz ^{17}O hyperfine coupling constants (Table S1, Supporting Information [SI]).[21−23] Consequently, the very small ^{17}O hyperfine coupling observed here indicates lack of direct Fe–O4 interaction, and most likely, the 3-CH$_2$^{17}OH group is rotated away from the unique fourth iron on reduction to [4Fe–4S]$^+$, as observed in crystal structures of a reduced (X-ray irradiated) wild-type IspH:**1**, as well as in a IspH E126Q:**1** complex.[24] This 3-CH$_2$OH rotated cyclic conformation is quite different to that found with the oxidized iron–sulfur cluster in which **1** forms the alkoxide complex (Intermediate I) containing an Fe–O bond.[4,5,15] These results indicate that the coordination of the 4-OH group to the [4Fe–4S] cluster is only involved in initial binding to the [4Fe–4S]$^{2+}$ oxidized cluster; following reduction, the 3-CH$_2$OH group has to rotate

dx.doi.org/10.1021/ja303445z | J. Am. Chem. Soc. 2012, 134, 11225–11234

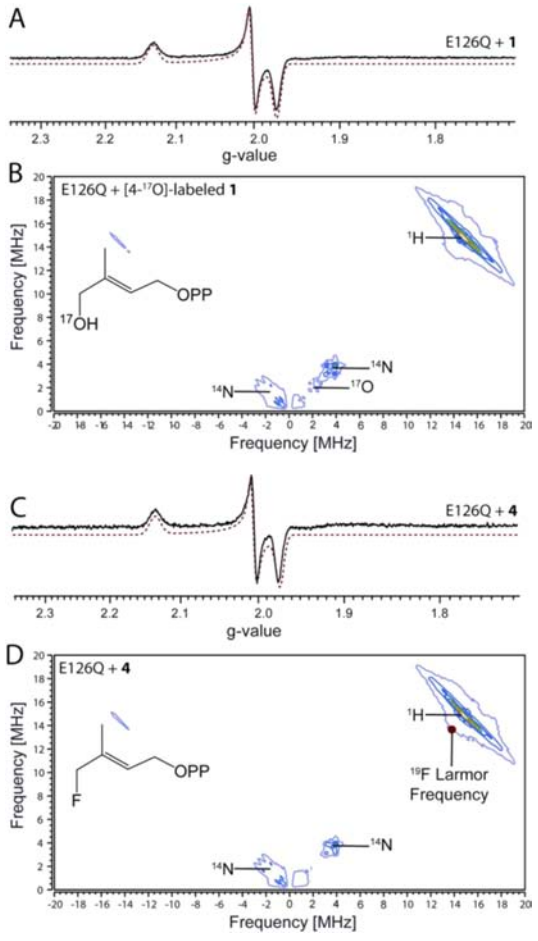

Figure 1. Binding of IspH substrate **1** and its fluoro analogue **4** to the E126Q mutant. (A) X-band EPR spectrum of E126Q + **1**. (B) X-band HYSCORE spectrum of E126Q + [4-^{17}O]-**1**. (C) X-band EPR spectrum of E126Q + **4**. (D) X-band HYSCORE spectrum of E126Q + **4**. Each HYSCORE spectrum is the sum of spectra taken at τ = 108, 136, and 208 ns, and was taken at g_2. T = 15 K. EPR spectral simulations are shown as red dotted lines.

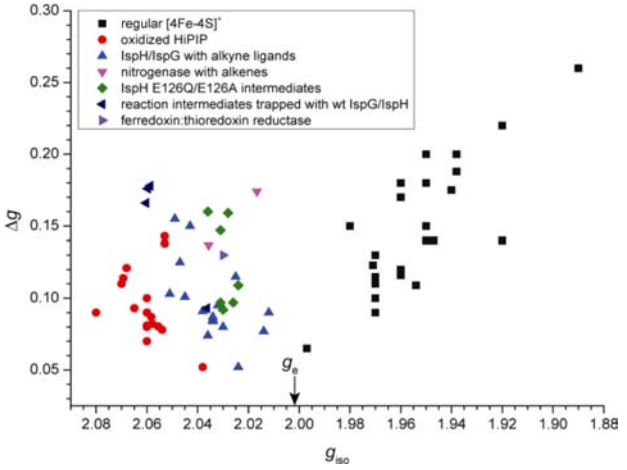

Figure 2. Plot of g_{iso} vs Δg for 80 iron–sulfur-containing systems. Free electron g-value is indicated by an arrow on the abscissa. Note that the three outliers in the oxidized HiPIP data points with coordinates (2.053, 0.138), (2.053, 0.142), and (2.038, 0.052) were from EPR signals of γ-irradiated single crystals, while most other data points were from samples in frozen solution. Please refer to Table S2, SI for details.

away in order to get protonated by the E126 residue and be removed.

What, then, might be some of the key interactions between the substrate **1** and the [4Fe–4S] cluster in this intermediate? Of note, intermediates II are characterized by rather unusual **g** tensors for $[4Fe–4S]^+$ clusters. Specifically, they have isotropic g-values ($g_{iso} = {}^1/_3(g_{11} + g_{22} + g_{33})$) of ~2.03–2.04, greater than the free electron g-value (g_e = 2.0023). Frequently, this is a characteristic of oxidized, high-potential iron–sulfur protein (HiPIP) clusters, $[4Fe–4S]^{3+}$, with more typical $[4Fe–4S]^+$ clusters having $g_{iso} < 2.0$.[25] In order to see if we might obtain additional insights into the nature of the bonding interactions in these intermediates, we compared **g** tensors of these complexes with those of a series of other [4Fe–4S] cluster-containing systems, Table S2 (SI [SI]). Among these are various ferredoxins, other [4Fe–4S] enzymes, synthetic models, typical HiPIPs, benzoyl CoA reductase, as well as IspG (HMBPP synthase) and IspH with alkene/alkyne ligands (EPR spectra are shown in Figure S1, SI). For ease of comparison, g_{iso} vs Δg ($g_{11} - g_{33}$) values are shown plotted in Figure 2. There appear to be three major clusters: (A) classic $[4Fe–4S]^+$ clusters[25] (black squares) where $g_{iso} < g_e$, from proteins such as ferredoxins, aconitase, and ligand-free IspH/IspG, as well as synthetic $[4Fe–4S]^+$ models, which contain primarily σ-bonded ligands. (B) Typical oxidized HiPIPs and synthetic $[4Fe–4S]^{3+}$ models (red circles), with $g_{iso} > g_e$. (C) $[4Fe–4S]^+$ clusters with alkene or alkyne ligands (blue triangles) where $g_{iso} > g_e$ but where these g_{iso}-values are generally smaller than those of typical HiPIPs. As can be seen in Figure 2, the reaction intermediates trapped with the IspH E126A/E126Q mutants belong to class C, which contain unsaturated ligands as in the nitrogenase–alkene complexes. These unusual HiPIP-like **g** tensors presumably reflect interactions between the metal cluster and the π-system of the ligand, where metal to ligand back-bonding would make the iron–sulfur clusters electron-deficient, similar to the conventional oxidized HiPIP clusters. In this context, the olefinic π-system of substrate **1** would then be the key structural element involved in interacting with the $[4Fe–4S]^+$ in this intermediate, rather than the 4-OH group.

We thus propose that this EPR-detected intermediate represents the 3-CH_2OH rotated π-complex/metallacycle (**7** or **8**, Intermediate II) proposed earlier[9] and directly observed recently by X-ray crystallography.[24] Considering that the Fe–C distances seen in the crystal structure[24] are longer than those observed in classical organometallic π-complexes or metallacycles, together with the fact that the C2–C3 carbons and their attached atoms are essentially planar, Intermediate II might best be described as the weak π- or van der Waals complex **7**.

Similar results were obtained with the 4-fluoro HMBPP analogue **4**. As shown in Figure 1C, the EPR spectrum of E126Q in the presence of **4** is essentially identical to the spectrum obtained with **1** (Figure 1A). This suggests two possibilities: one is that when bound to IspH, the fluorine of **4** hydrolyzes to afford **1**; a second possibility is that the 3-CH_2F group in **4** rotates away from the $[4Fe–4S]^+$, just as the 3-CH_2OH group in **1** does. Both possibilities are consistent with the ^{19}F-HYSCORE result of E126Q + **4** (Figure 1D) taken at three different τ-values, which show no evidence of any ^{19}F hyperfine interaction—an observation that also rules out the Fe–F bonding present in some models.[16]

A New Intermediate Is Trapped with Wild-Type IspH and Is Assigned to Intermediate III. We next studied the

reactions of **1** and **4** with wild-type IspH by freeze-quench EPR experiments. In a typical reaction, 30 equiv of $Na_2S_2O_4$ and 10 equiv of substrates were added, and no electron mediator (e.g., methyl viologen) was used. Under these conditions, the reaction should last about 30 min, since we found by using an NMR assay that the specific activity is $\sim 10^3$ times slower than that when methyl viologen was used as an electron mediator. By freeze quenching the reaction at 30 s, a new paramagnetic reaction intermediate was trapped using either **1** or **4**, both characterized by **g** = [2.171, 2.010, 1.994] (Figure 3A,B)—a **g** tensor different from those observed with

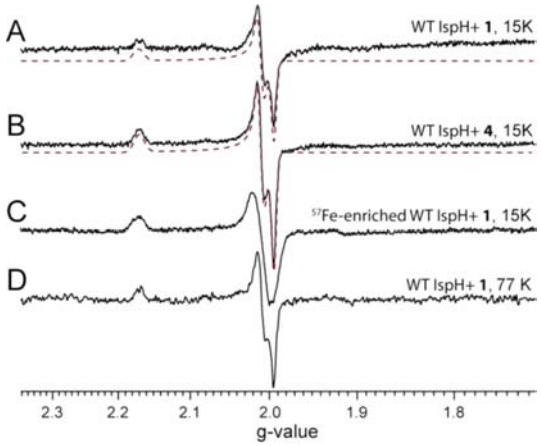

Figure 3. X-band EPR spectra of the reaction intermediate trapped with wild-type IspH. (A) IspH + **1** at 15 K. (B) IspH + **4** at 15 K. (C) ^{57}Fe-enriched IspH + **1** at 15 K. (D) IspH + **1** at 77 K. Spectral simulations are shown as red dotted lines.

intermediates II trapped by IspH E126A/E126Q mutants. This intermediate lasted at least 25 min in the absence of an electron mediator, consistent with the slow reaction rate under this condition; after 40 min incubation, it disappeared and only a product isopentenyl diphosphate/dimethylallyl diphosphate (IPP/DMAPP)-bound IspH signal was detected (Figure S2A, SI). In the presence of one equivalent of methyl viologen, the reaction intermediate almost disappeared ~5 s after mixing *E. coli* IspH with 120 equiv of $Na_2S_2O_4$ and 50 equiv of **1** (Figure S2B, SI), consistent with the much faster reaction rate when methyl viologen is used as the electron mediator (specific activity =16.3 μmol·min^{-1}·mg^{-1}, or k_{cat} = 9.8 s^{-1}).[3]

One possibility with the native protein is that this species represents the next reaction intermediate in the proposed pathway, Intermediate III in Scheme 2, since in the presence of a native E126, the 4-OH group of **1** (or the fluorine of **4**) can be protonated and removed, forming the paramagnetic Intermediate III. The results of ^{17}O- and ^{19}F-HYSCORE experiments on this intermediate, prepared by using [4-^{17}O]-**1** or **4** (Figure 4A,B), gave no evidence for either ^{17}O or ^{19}F hyperfine interactions, respectively. This is consistent with an assignment to Intermediate III in Scheme 2. This intermediate is likely the η^3-allyl complex **10** observed crystallographically, and has Fe−C distances (2.6−2.7 Å) that are shorter than the sum of van der Waal radii (3.6 Å) of iron and carbon.[5] This crystallographically observed species is less likely to be either **2** or **3**, since soaking of IspH:**1** crystals with a mixture of sodium dithionite and methyl viologen leads to decomposition,[24] while soaking of the inactive E126Q mutant crystals bound to **1** does not. This indicates that upon product formation, IspH

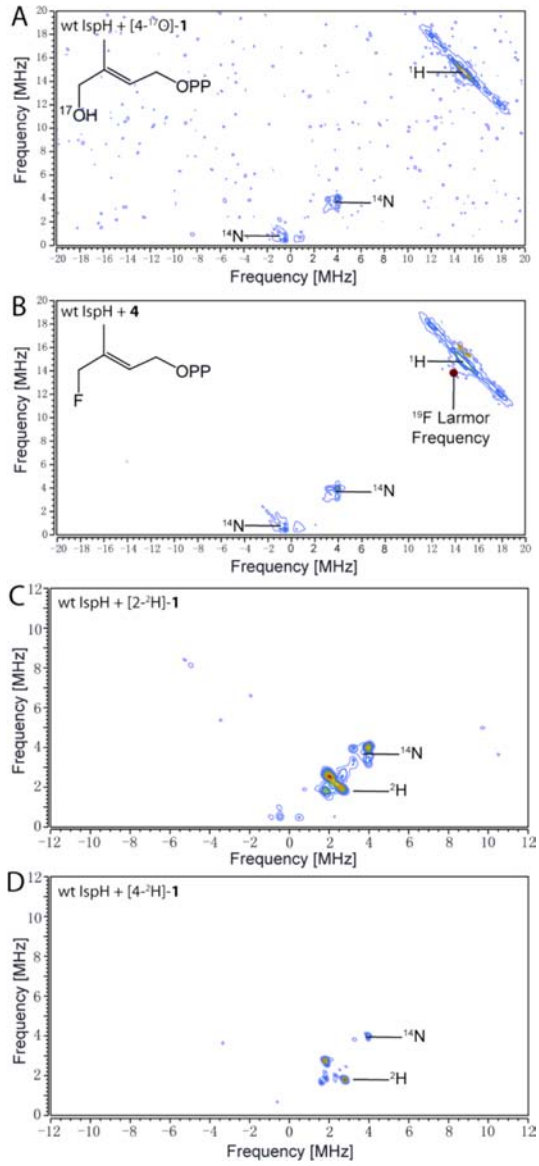

Figure 4. X-band HYSCORE spectra of the reaction intermediate trapped with wild type IspH. (A), IspH + [4-^{17}O]-**1**. (B), IspH + **4**. (A) and (B) are sums of spectra taken at τ = 108 ns, 136 ns, and 208 ns. (C), IspH + [2-^{2}H$_1$]-**1**. (D), IspH + [4-^{2}H$_1$]-**1**. τ = 136 ns. (A−D) were collected at g_2.

undergoes structural rearrangements to release the products, which disturb the crystal packing and result in decomposition of the crystal.

However, are there other structural possibilities for Intermediate III and its role in catalysis? Is it possible that this intermediate is the allyl radical **14** in the Birch reduction-like mechanism? It seems unlikely that this species arises from a carbon-based radical, for the following reasons. First, the **g** tensor is highly anisotropic, while typical organic radicals have isotropic **g** tensors. Second, the EPR line width is significantly broadened with ^{57}Fe-enriched IspH (Figure 3C) due to unresolved ^{57}Fe hyperfine couplings, indicating that most of the spin density is on the [4Fe−4S] cluster. Third, the intermediates prepared from [2-^{2}H$_1$]-**1** or [4-^{2}H$_1$]-**1** have only small deuterium hyperfine coupling constants ($A_y(^2H) \approx 0.5$ and 0.9 MHz, respectively, or 3.2 and 5.9 MHz in terms of $A_y(^1H)$, Figure 4C,D), much smaller than those of allyl radicals

dx.doi.org/10.1021/ja303445z | J. Am. Chem. Soc. 2012, 134, 11225−11234

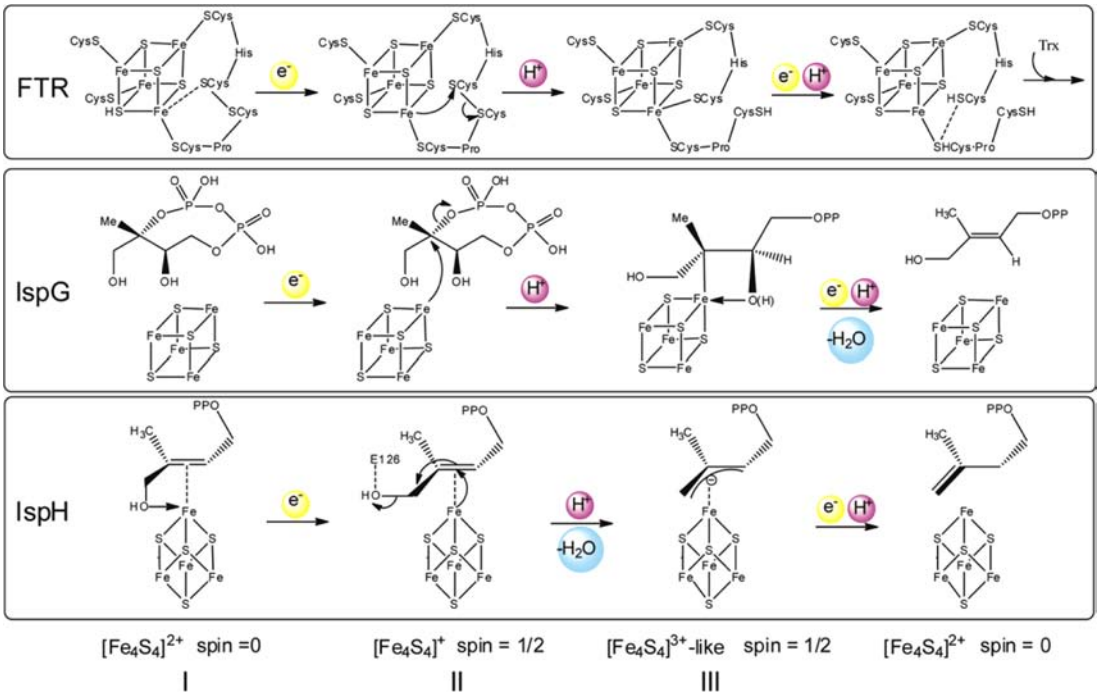

Figure 5. Unified reaction mechanisms of FTR, IspG, and IspH.

($A(^1H) \approx 14$ G, or 39 MHz).[26] These results suggest that this species is not a radical.

However, neither does it have an EPR spectrum characteristic of most $[4Fe-4S]^+$ clusters. The g_{iso}-value of Intermediate III is 2.06, greater than the free electron g-value ($g_e = 2.0023$), and the **g** tensor is more akin to that seen in HiPIP proteins.[25] Unlike Intermediate II, which we propose is a weak π-complex formed between the unreactive E126Q mutant and the alkene **1**, Intermediate III was trapped under turnover conditions. How, then, might a $[4Fe-4S]^{3+}$-like cluster be generated during catalysis? Notably, quite similar spectra have been found with other $[4Fe-4S]$ proteins catalyzing $2H^+/2e^-$ reductions. For example, in both IspG[27,28] and ferredoxin:thioredoxin reductase (FTR),[29−31] EPR spectra of reaction intermediates are characterized by $g_{iso} > 2$. In addition, the EPR signals have unusual relaxation properties, being observable without broadening at 77 K or even higher temperatures. The same result is also observed with IspH Intermediate III (Figure 3D).

FTR is a well-characterized system, and it is thought that its $[4Fe-4S]^{2+}$ cluster undergoes a one-electron reduction followed by a two-electron reduction of a disulfide bond, yielding a HiPIP-type $[4Fe-4S]^{3+}$ cluster, thus avoiding generation of a thiol free radical.[30,31] As shown in Figure 5, the IspG as well as IspH catalytic mechanisms can all be cast in essentially the same manner as proposed for FTR catalysis. In each case, following a one-electron reduction of the $[4Fe-4S]^{2+}$ cluster (Intermediate I), the resulting $[4Fe-4S]^+$ (Intermediate II) carries out a formally two-electron reduction of its substrate, generating an oxidized HiPIP-like cluster $[4Fe-4S]^{3+}$ (Intermediate III). Although intermediates III in Figure 5 have resonance forms as diamagnetic $[4Fe-4S]^{2+}$ clusters with free-radical ligands (**14** and **16**, Scheme 4), as discussed above and elsewhere,[9,32,33] the experimental results are inconsistent with these intermediates being radicals. On the basis of these observations, the Birch reduction-like catalytic mechanism with radical intermediates[7,16,17] again seems rather unlikely.

Scheme 4. Resonance Forms Proposed for Intermediates in IspG and IspH Catalyses; (A) Allyl Anion 9 /Radical 14 in IspH Catalysis; (B) Ferraoxetane 15 /Radical 16 in IspG Catalysis (note the corresponding changes in cluster charge)

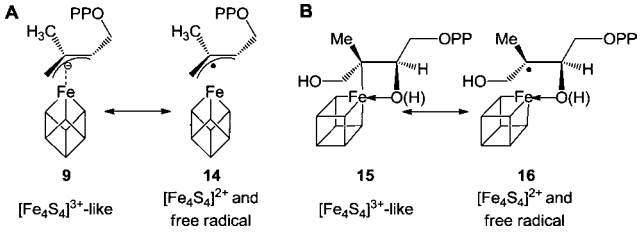

The Birch reduction-like mechanism,[16,17] then, does not fit current experimental results because of the following four reasons: (i) In the Birch reduction-like mechanism, the 4-OH group binds to the reduced $[4Fe-4S]^+$ cluster in **12** and is protonated by the T167 hydroxyl group in **13**. This contradicts the results of a computational docking study,[9] a crystal structure of an IspH:**1** complex,[24] the ^{17}O-HYSCORE data on Intermediate II presented here, and a recent report using deuterated compounds on the stereochemical course of IspH catalysis.[18] These results all indicate or support the idea that after initial alkoxide complex **6** formation, on reduction the 3-CH_2OH group rotates away from the iron−sulfur cluster. This rotation enables the 4-OH group to be protonated by the carboxyl group of E126, which is more acidic than the hydroxyl group of T167. This protonation facilitates the dehydration of **1**. (ii) There are two distinct radical species involved in the Birch reduction-like mechanism. However, neither has been observed. The paramagnetic intermediate trapped with wild-type IspH is likely to be an η^3-allyl complex; however, its **g** tensor, the deuterium hyperfine coupling constants, and the ^{57}Fe broadening effect all indicate this intermediate is not a typical organic radical. (iii) The Birch reduction-like mechanism cannot explain the identities of the paramagnetic

dx.doi.org/10.1021/ja303445z | J. Am. Chem. Soc. 2012, 134, 11225−11234

intermediates trapped with either wild-type IspH or the E126Q mutant. As discussed above, these intermediates are not radicals and thus cannot be either **13** or **14**; they cannot be intermediate **12** either, because no sizable ^{17}O hyperfine coupling signal is observed. These paramagnetic intermediates also of course cannot be **6** or **11′**, since these are diamagnetic. (iv) Finally, the cluster-bound water molecule in **11′** and **14** is not observed in the crystal structure of the η^3-allyl complex.[5]

***iso*-HMBPP (5) Follows the Same Reaction Mechanism As Does HMBPP (1).** We next investigated the reaction of IspH with its substrate analogue, *iso*-HMBPP (**5**). Previous workers found that [5-$^{13}C_1$]-**5** only afforded one product, **17**; **17′** was not detected (Scheme 5).[17] On the basis of this result,

Scheme 5. Reaction of 5 with IspH

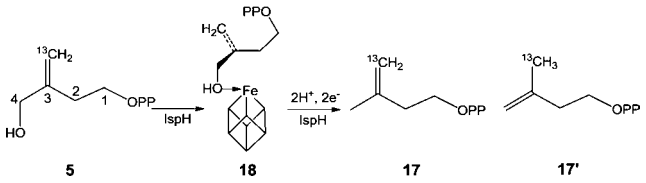

the following three proposals were made: (i) **17** as the only product was due to the formation of the alkoxide complex **18**, which positioned the C5 carbon away from the proton source, the diphosphate oxygen, so C5 was not protonated in the reaction; (ii) this result indicated the π-bond of **5** is far away from the iron−sulfur cluster, so the interaction between the π-bond of **5** and the iron−sulfur cluster was not involved in catalysis; and (iii) the two electrons were delivered one after another (Birch reduction-like mechanism), generating distinct organic free radical intermediates.[16,17] To test these hypotheses, we obtained the structure of the IspH:**5** complex (PDB code 4EB3). In addition, we studied the reaction using EPR spectroscopy. The results do not support the radical mechanism, for the following reasons.

First, although the initial intermediate, the alkoxide complex **18** was indeed observed (Figure 6A, B), this is as expected and does not provide any information on π-interactions in subsequent reactions. As with the natural substrate **1**, on reduction of the iron−sulfur cluster, the presence of a π-interaction is supported by the EPR spectrum of IspH E126Q + **5** (Figure 6C) which shows two components, characterized by $\mathbf{g}_1$ = [2.091, 1.999, 1.999] with $g_{iso,1}$ = 2.030; and $\mathbf{g}_2$ = [2.091, 1.999, 1.982] with $g_{iso,2}$ = 2.024. The g_{iso}-values of E126Q + **5** are greater than g_e, and fall in the type C region in Figure 2. This result suggests that on cluster reduction, the 3-CH_2OH group of **5** rotates away just as it does with **1**, so that the C=C can come closer to the [4Fe−4S]$^+$ cluster and interact with the unique fourth iron.

Second, the formation of the initial alkoxide complex **18** does not suggest a Birch reduction-like mechanism. As with **1**, we trapped a reaction intermediate using wild-type IspH. The EPR spectrum was characterized by **g** = [2.171, 2.005, 2.005] (Figure 6D), very similar to the **g** tensor of the intermediate trapped with **1**, which we have assigned to the η^3-allyl complex having an oxidized HiPIP-like cluster (Intermediate III). This suggests that—as with **1**—the one-electron reduction of the IspH [4Fe−4S]$^{2+}$ cluster is followed by a formal two-electron reduction of **5**, yielding a HiPIP-type [4Fe−4S]$^{3+}$ cluster (in Intermediate III′), with no distinct organic radicals observed. Taken together, these results indicate that **5** follows the same reaction mechanism as does the natural substrate **1**, as shown in Scheme 6.

Scheme 6. Reaction Mechanism of IspH with 5 Is the Same as with 1

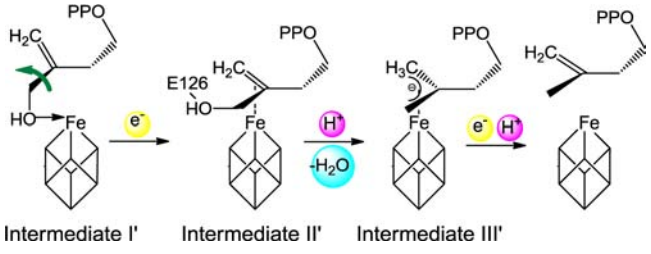

Why, then, is **17**, the sole product of **5**, reacting with IspH? Our results indicate that this is not due to the absence of a π-interaction, or to a radical reaction mechanism. It only indicates the proton source in the final protonation step, the diphosphate oxygen, is closer to C4 than C5, which is indeed suggested by the crystal structure of the IspH:**5** complex (Figure 6B). This crystal structure also provides a ready explanation as to why the K_m of **5** is 35-fold larger than that of **1**[17]; the average Fe−C3 and Fe−C5 distance in the alkoxide complex formed by **5** is 0.5 Å longer than that seen in the alkoxide complex formed by **1**.[5] Thus, the π-interaction does not contribute much to the initial binding of **5**. However, as suggested by the EPR results (Figure 6C,D), C3 and C5 of **5** are likely to move closer to the iron−sulfur cluster on reduction, with the π-interaction playing an important role in the later catalytic steps, just as with **1**.

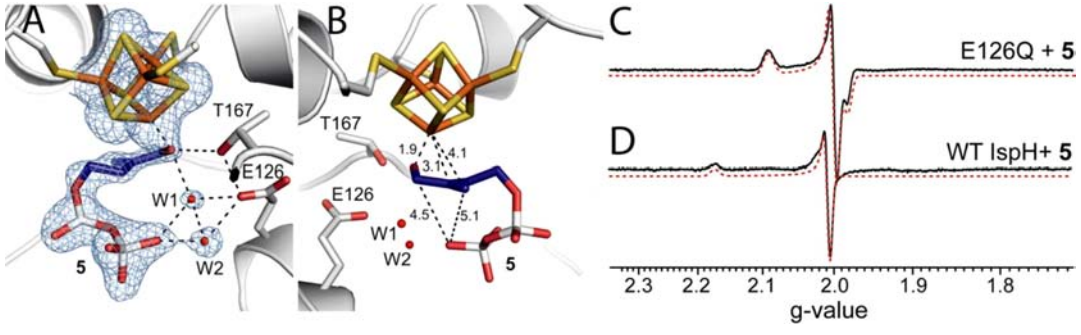

Figure 6. *iso*-HMBPP (**5**) binding to and reacting with *E. coli* IspH. (A and B) X-ray structure of the alkoxide complex formed by IspH + **5**. Electron densities in (A) represented in blue are contoured at 1.0σ with $2F_0$-F_c coefficients. C4−O, C5−O, Fe−C3, and Fe−C5 distances are labeled in Å in (B). (C) X-band EPR of IspH E126Q mutant + **5**. (D) X-band EPR of wild-type IspH + **5**. Spectral simulations are shown as red dotted lines.

dx.doi.org/10.1021/ja303445z | *J. Am. Chem. Soc.* 2012, 134, 11225−11234

A Ferraoxetane as an IspH Reaction Intermediate Is Also Unlikely. After submission of this manuscript, the formation of the $g_1 = 2.17$ reaction intermediate (Intermediate III in our mechanism) was reported by others.[34] They noted the HiPIP-like nature of the iron–sulfur cluster, but proposed an alternative possibility: that this species contains a ferraoxetane ring, i.e. a structure containing an Fe–O bond (**19**, Scheme 7A). This structure is reminiscent of that we

Scheme 7. (A) Proposed Ferraoxetane Structure As IspH Reaction Intermediate; (B) IspH Ferraoxetane Mechanism for Reaction with Substrate Analogue 5

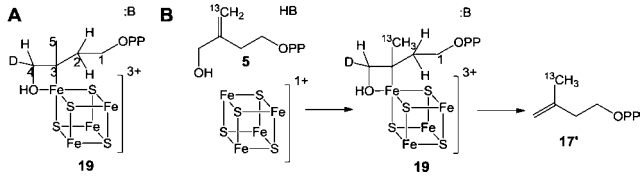

proposed for the reaction intermediate "X" of another [4Fe–4S] enzyme, IspG.[28,32,33,35] However, the involvement of a ferraoxetane in the IspH reaction seems unlikely, for the following five reasons.

First, we do not find any ^{17}O hyperfine interaction with the $g_1 = 2.17$ IspH reaction intermediate (Figure 4A), while a large ^{17}O hyperfine coupling (~9 MHz) was found in the IspG reaction intermediate "X",[32] quite close to the mean value of $A(^{17}O) = 8.9$ MHz found in H_2O or HO^- bound to the Fe_a site of aconitase (Table S1, SI).[22,23] The lack of any ^{17}O hyperfine interaction makes the involvement of such a ferraoxetane intermediate in IspH catalysis rather unlikely. Second, in the IspH ferraoxetane mechanism, there is no involvement of the 3-CH_2OH group rotation seen crystallographically[24] as well as deduced from isotope-labeling studies of the product IPP (**2**) C4 H_E, H_Z-stereochemistry, which requires such a rotation.[18] Third, C2 is protonated in the proposed ferraoxetane **19**, which will lead to the formation of only IPP, not a mixture of DMAPP and IPP. Fourth, the observation that the fluoro substrate analogue **4** can react with IspH and forms the same intermediate as that seen with the natural substrate **1** is also inconsistent with an assignment to a ferraoxetane species for Intermediate III, because **4** does not have a hydroxyl group. Fifth, the IspH ferraoxetane mechanism is inconsistent with the observation that **17** is the only product of **5** reacting with IspH. Rather, this mechanism would predict **17′** being the product (Scheme 7B). In addition, if **5** does react via a ferraoxetane intermediate, it should be the same as the ferraoxetane formed from **1**. However, the observed *g*-values of these two intermediates are similar but not the same (compare Figure 3A with Figure 6D).

Thus, the IspH ferraoxetane mechanism is either inconsistent with several experimental results, or suggests substrate analogues **4** and **5** would react through completely different mechanisms. In this context, the bioorganometallic mechanism proposed here is preferred since it is consistent with all the experimental observations with **1**, **4**, and **5**. In a brief summary, Table 1 compares the three proposed mechanisms from six different perspectives.

■ CONCLUSIONS

The results reported here support the bioorganometallic mechanism of IspH catalysis. There are two paramagnetic

Table 1. Comparison between Prediction and Experiment for Three Proposed IspH Catalytic Mechanisms

	experimental results					
	crystallography (ref 24) and ^2H-labeling (ref 18) indicate 3-CH_2OH group rotates during reaction	very small 4-^{17}O hyperfine coupling observed for the intermediate trapped with E126Q/A (this study)	no 4-^{17}O hyperfine coupling observed for the intermediate trapped with WT IspH (this study)	**g**-tensor of the intermediate trapped with WT IspH (ref 34 and this study)	DMAPP formation	reactions with substrate analogues **4**, **5** (refs 16, 17 and this study)
Birch reduction-like mechanism (refs 16, 17)	inconsistent; no rotation involved	inconsistent; direct Fe–O bonding in **12** would lead to a large ^{17}O coupling	inconsistent; cannot be **12** which has a Fe–O bond; cannot be **13** or **14**, since these radicals would have more isotropic **g**-tensors	consistent with HiPIP-like cluster	consistent	inconsistent with nonradical **g**-value of reaction intermediates
IspH ferraoxetane mechanism (ref 34)	inconsistent; no rotation involved	N/A; mechanism considers this species to be a dead-end product	inconsistent; Fe–O bond in ferraoxetane would give a large ^{17}O coupling	consistent with HiPIP-like cluster	inconsistent; no route to DMAPP	inconsistent; cannot explain reactions with **4**, **5**
bio-organometallic mechanism (this study)	consistent; 3-CH_2OH group rotates in this mechanism	consistent; 3-CH_2OH group rotates away in Intermediate II; no direct Fe–O bonding	consistent; 4-OH group has been removed, forming Intermediate III	consistent with HiPIP-like cluster	consistent	consistent; explains reactions with **4**, **5**

dx.doi.org/10.1021/ja303445z | J. Am. Chem. Soc. 2012, 134, 11225–11234

reaction intermediates proposed in this mechanism, and two have been trapped and characterized here. The intermediate trapped with IspH E126A/E126Q mutants represents the 3-CH_2OH-rotated weak π-complex, Intermediate II. Following a formal two-electron reduction and dehydration of the substrate, Intermediate II is converted into an η^3-allyl complex with an oxidized HiPIP-like cluster $[4Fe{-}4S]^{3+}$, Intermediate III, which we have now observed with wild-type IspH. Two similar paramagnetic intermediates were obtained with the substrate analogues **4** and **5**, indicating they also follow the same bioorganometallic reaction mechanism as that of **1**. This reaction mechanism (as well as that of IspG) has close similarities to that proposed for the ferredoxin−thioredoxin reductase reaction in which oxidized HiPIP-like intermediates, but not distinct organic free radicals, are involved. The two paramagnetic intermediates reported here do not fit the Birch reduction-like mechanism while all available EPR, Mössbauer, computational docking, crystallographic, and stereochemical results are consistent with the bioorganometallic model for IspH catalysis. We also note that a ferraoxetane model of IspH Intermediate III reported during the review of this manuscript is inconsistent with several experimental observations.

MATERIALS AND METHODS

Protein Expression. Wild type *E. coli* IspH or the E126Q mutant with a Strep-tag[36] (encoded in plasmid pASK-IBA3$^+$) were coexpressed with *isc* proteins (encoded in plasmid pDB1282) in BL-21(DE3) cells. LB media was supplemented with 100 mg/L ampicillin and 50 mg/L kanamycin. Cells were initially grown at 37 °C; when the OD_{600} reached 0.3, cells were induced with 0.5 g/L arabinose to initiate overexpression of the *isc* proteins. Cysteine (1 mM) and $FeCl_3$ (0.1 mM) were supplemented and cells grown until the OD_{600} reached 0.6. At this point, 400 μg/L anhydrotetracycline was added to induce overexpression of *E. coli* IspH. Cells were grown at 25 °C for 16 h, harvested by centrifugation, and kept at −80 °C until use.

Purification of Wild-Type IspH. All purification steps were carried out in a Coy Vinyl Anaerobic Chamber (Coy Laboratories, Grass Lake, MI) with an oxygen level <2 ppm, and all buffers were degassed by using a Schlenk line. Cell pellets were resuspended in 100 mM Tris-HCl, 150 mM NaCl buffer (pH 8.0). Lysozyme, Benzonase nuclease (EMD Chemicals, San Diego, CA) and phenylmethanesulfonyl fluoride were added, and stirred for one hour at 10 °C followed by sonication (Fisher Scientific Sonic Dismembrator, model 500) with four pulses, each 7 s duration, at 35% power. The cell lysate was centrifuged at 11,000 rpm at 10 °C for 30 min. The supernatant was purified by using Strep-tactin chromatography.[36] Fractions having a brown color were collected and desalted in pH 8.0 buffer containing 100 mM Tris-HCl and 150 mM NaCl.

Purification of the IspH E126Q Mutant. The Strep-tagged IspH E126Q mutant purified according to the above protocol had bound HMBPP (**1**), as evidenced by the EPR spectrum of the as-purified enzyme. In order to obtain substantially HMBPP-free E126Q, the purification protocol was modified. Basically, His-tagged wild type *A. aeolicus* IspH was added to the cell lysate to 20 μM. Sodium dithionite was also added to ∼3−6 mM. The cell lysate was then incubated with stirring for ∼2 h, during which time the wild type IspH converted HMBPP into IPP/DMAPP, which have weaker binding affinity to IspH E126Q. Finally, the cell lysate was centrifuged and the supernatant purified by using Strep-tactin chromatography. The resulting E126Q protein had only ∼10% HMBPP bound, as measured by EPR spectroscopy.

EPR Spectroscopy. EPR data were obtained as described previously.[33] Spectra were simulated using EasySpin.[37]

Crystallization. *E. coli* IspH protein for crystallization was prepared as reported previously.[14] Co-crystallization of IspH with **5** was performed under anaerobic conditions in a Coy Vinyl Anaerobic Chamber with an N_2/H_2 (95%/5%) atmosphere. All buffers were refluxed for 20 min and stored under argon. A 100 mM aqueous solution of **5** was prepared under anaerobic conditions. A 18.3 mg/mL IspH solution was incubated with 5 mM **5** prior to crystallization. Brown crystals were obtained by using the sitting drop vapor diffusion method at 20 °C with 100 mM Bis Tris/HCl, pH 6.5, 200 mM ammonium sulfate and 25% polyethylene glycol 3350 as precipitant. Crystals were soaked with cryoprotectant (50% aqueous polyethylene glycol 400) for 1 min, mounted on loops, and flash cooled in a stream of nitrogen gas at 100 K (Oxford Cryo Systems).

Data Collection and Structure Determination. Native data sets were collected using synchrotron radiation at the X06SA-beamline at the Swiss Light Source, Villigen, Switzerland. The phase problem was solved by molecular replacement using the coordinates of *E. coli* IspH bound to HMBPP (PDB ID: 3KE8) as the starting model.[14,38] Data were processed using the program package XDS.[39] The anisotropy of diffraction was corrected using TLS refinement.[40] Model building and refinement were performed with Coot[41] and Refmac.[42] Water molecules were fitted automatically with ARP/wARP.[43] Figures were prepared using PyMOL,[44] and Ramachandran plots were calculated with PROCHECK.[45] For more details see Table S3, SI.

Accession Number. The atomic coordinates for IspH in complex with **5** have been deposited in the Protein Data Bank, Research Collaboratory for Structural Bioinformatics at Rutgers University, PDB ID 4EB3.

Synthetic Aspects. General Methods. All reagents used were purchased from Aldrich (Milwaukee, WI). The purity of all compounds investigated was confirmed by using ^1H and ^{31}P NMR spectroscopy at 400 MHz on Varian (Palo Alto, CA) Unity spectrometers. Cellulose TLC plates were visualized by using iodine or a sulfosalicylic acid−ferric chloride stain.

*[^{17}O]-2-Methyl-2-vinyloxirane (**20**).* To a stirred mixture of isoprene (1.36 g, 20 mmol) and N-bromosuccinimide (178 mg, 1 mmol) was added $H_2{}^{17}O$ (72 mg, 4 mmol) at 4 °C. The mixture was stirred vigorously at that temperature for 10 h and then filtered and washed with hexane (5 mL × 4). The filtrate was dried with anhydrous Na_2SO_4 and then evaporated under reduced pressure. The residue was dissolved in 7 mL of CH_2Cl_2, and 2 mL of ammonium hydroxide added. The mixture was then stirred vigorously at room temperature for 4 h. The organic layer was separated and dried with anhydrous Na_2SO_4 and then concentrated by careful evaporation of the CH_2Cl_2 to a pale-yellow liquid that was used for the next step without further purification (Scheme 8). ^1H NMR (400 MHz, $CDCl_3$): δ 1.43 (s, 3H), 2.70 (d, J = 5.0 Hz, 1H), 2.79 (d, J = 5.0 Hz, 1H), 5.20 (d, J = 10.5 Hz, 1H), 5.33 (d, J = 17.5 Hz, 1H), 5.58−5.63 (m, 1H).

Scheme 8. Synthesis of [4-17O]-1[a]

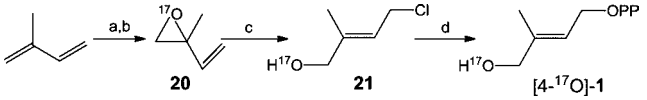

[a](a) NBS, $H_2{}^{17}O$, 0°C; (b) $NH_3{\cdot}H_2O$; (c) $TiCl_4$, −90°C; (d) $(n\text{-}Bu_4N)_3HP_2O_7$, CH_3CN.

*(E)-4-Chloro-2-methylbut-2-en-1[^{17}O]-ol (**21**).* (*E*)-4-Chloro-2-methylbut-2-en-1[^{17}O]-ol was synthesized according to a literature method.[46] To a solution of $TiCl_4$ (285 mg, 1.5 mmol) in 3 mL of dry CH_2Cl_2 was added a solution of [^{17}O]-2-methyl-2-vinyloxirane (85 mg, 1 mmol)) in 0.5 mL of dry CH_2Cl_2 at −90 °C under an atmosphere of nitrogen. The reaction mixture was stirred at that temperature for 2 h, then quenched using 5 mL of 1 N HCl. The organic layer was separated and the aqueous layer extracted with ether (5 mL × 4). The combined organic phase was dried with anhydrous Na_2SO_4 and then evaporated under reduced pressure. The residue was purified by flash silica chromatography (hexane/EtOAc = 3:2) to yield 56 mg (46%) of a colorless oil. ^1H NMR (400 MHz, $CDCl_3$): δ 1.70 (s, 3H), 4.02 (s, 2H), 4.09 (d, J = 8.0 Hz, 2H), 5.62−5.72 (m, 1H).

(E)-4[^{17}O]-Hydroxy-3-methyl-2-butenyl Diphosphate ([4-^{17}O]-1). (*E*)-4[^{17}O]-Hydroxy-3-methyl-2-butenyl diphosphate was synthesized

according to a literature method.[9,47] (*E*)-4-Chloro-2-methylbut-2-en-1[^{17}O]-ol (24 mg, 0.2 mmol) was added dropwise to a stirred solution of 0.45 g (0.5 mmol) tris(tetra-*n*-butylammonium) hydrogen diphosphate in CH_3CN (1.5 mL) at 0 °C; the reaction mixture was slowly allowed to warm to room temperature over 2 h, and then solvent was removed under reduced pressure. The residue was dissolved in 0.5 mL of cation-exchange buffer (49:1(v/v) 25 mM NH_4HCO_3/2-propanol) and passed over 90 mequiv of Dowex AG50W-X8 (100−200 mesh, ammonium form) cation-exchanged resin pre-equilibrated with two column volumes of the same buffer. The product was eluted with two column volumes of the same buffer, flash frozen, and lyophilized. The resulting powder was dissolved in 0.5 mL of 50 mM NH_4HCO_3. 2-Propanol/CH_3CN (1:1 (v/v), 1 mL) was added, the mixture vortexed, and then centrifuged for 5 min at 2000 rpm. The supernatant was decanted. This procedure was repeated three times, and the supernatants were combined. After removal of the solvent and lyophilization, a white solid was obtained. Flash chromatography on a cellulose column (53:47(v/v) 2-propanol/50 mM NH_4HCO_3) yielded 22 mg (35%) of a white solid. ^{1}H NMR (400 MHz, D_2O) δ 1.53 (s, 3H), 3.84 (s, 2H), 4.35 (t, J = 7.2 Hz, 2H), 5.45−5.51 (m, 1H); ^{31}P NMR (162 MHz, D_2O) δ −9.71 (d, J = 20.7 Hz), −8.92 (d, J = 20.7 Hz).

*Methyl 4-Bromo-2-methylenebutanoate (**22**).* Hydrogen bromide was passed through an ice-cooled solution of 3-methylenedihydro-2(3*H*)-furanone (0.98 g, 10 mmol) in methanol (5 mL). The mixture was allowed to stand at room temperature overnight and then heated at 60 °C for 5 h. The mixture was poured into brine and extracted with ether (10 mL × 4). The organic layer was separated and dried with anhydrous Na_2SO_4. After the solvent was evaporated under reduced pressure, the residue was purified by flash silica chromatography (hexane/EtOAc = 5:1) to yield 87 mg (45%) of a colorless oil. ^{1}H NMR (400 MHz, $CDCl_3$) δ 2.84 (t, J = 6.8 Hz, 2H), 3.51 (t, J = 6.8 Hz, 2H), 3.75 (s, 3H), 5.67 (s, 1H), 6.28 (s, 1H).

*[1,1-$^2H_2$]-4-Bromo-2-methylenebutan-1-ol (**23**).* To a mixture of $LiAlD_4$ (42 mg, 1 mmol) in dry ether (10 mL) at 0 °C, was added dropwise a solution of methyl 4-bromo-2-methylenebutanoate (**1**) (190 mg, 1 mmol) in dry ether (2 mL). The mixture was stirred for 2 h. After the reaction was quenched at 0 °C by addition of a few drops of water, precipitates were removed by filtration and washed with ether (5 mL × 4). The filtrate was dried with anhydrous Na_2SO_4 and then evaporated under reduced pressure. The residue was purified by flash silica chromatography (hexane/EtOAc = 2:1) to yield 55 mg (33%) of a colorless oil. ^{1}H NMR (400 MHz, $CDCl_3$): δ 2.64 (t, J = 7.2 Hz, 2H), 4.96 (s, 1H), 5.14 (s, 1H) (see Scheme 9).

Scheme 9. Synthesis of [4-$^2H_2$]5[a]

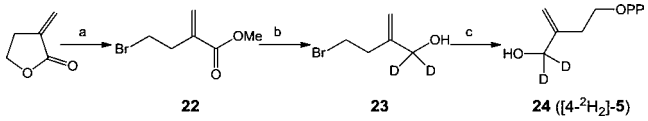

[a](a) HBr(g), MeOH; (b) $LiAlD_4$, 0°C; (c) (n-Bu_4N)$_3HP_2O_7$, CH_3CN, 0°C.

*[4,4-$^2H_2$]-4-Hydroxy-3-methylenebutyl Diphosphate (**24**).* [1,1-$^2H_2$]-4-Bromo-2-methylenebutan-1-ol (33 mg, 0.2 mmol) was added dropwise to a stirred solution of 0.45 g (0.5 mmol) of tris(tetra-*n*-butylammonium) hydrogen diphosphate in CH_3CN (1.5 mL) at 0 °C, and the reaction mixture was slowly allowed to warm to room temperature over 2 h. The solvent was removed under reduced pressure. The residue was dissolved in 0.5 mL of cation-exchange buffer (49:1 (v/v) 25 mM NH_4HCO_3/2-propanol) and passed over 90 mequiv of Dowex AG50W-X8(100−200 mesh, ammonium form) cation-exchanged resin pre-equilibrated with two column volumes of the same buffer. The product was eluted with two column volumes of the same buffer, flash frozen, and lyophilized. The resulting powder was dissolved in 0.5 mL of 50 mM NH_4HCO_3. 2-Propanol/CH_3CN (1: 1 (v/v), 1 mL) was added, the mixture was vortexed and then centrifuged for 5 min at 2000 rpm. The supernatant was decanted. This procedure was repeated three times, and the supernatants were combined. After removal of the solvent and lyophilization, a white solid was obtained. Flash chromatography on a cellulose column (53:47 (v/v) 2-propanol/50 mM NH_4HCO_3) yielded 23 mg (37%) of a white solid. ^{1}H NMR (400 MHz, D_2O) δ 2.22 (t, J = 6.4 Hz, 2H), 3.86 (q, J = 6.4 Hz, 2H), 4.85 (s, 1H), 4.92 (s, 1H); ^{31}P NMR (162 MHz, D_2O) δ −9.87 (d, J = 20.7 Hz), −9.04 (d, J = 20.7 Hz).

■ ASSOCIATED CONTENT

Supporting Information

Tables S1−S3 and Figures S1 and S2. This material is available free of charge via the Internet at http://pubs.acs.org.

■ AUTHOR INFORMATION

Corresponding Author

eo@chad.scs.uiuc.edu

Notes

The authors declare no competing financial interest.

■ ACKNOWLEDGMENTS

This work was supported by the TUM Graduate School, the Hans-Fischer Gesellschaft, DFG Grant GR1861/5-1, NIH Grant GM65307, and American Heart Association Predoctoral Fellowship 10PRE4430022. We thank Pinghua Liu for providing the *E. coli* IspH expression system, Hassan Jomaa and Jochen Wiesner for providing the *A. aeolicus* IspH expression system, and Dennis Dean for providing the *isc* protein expression system. We also thank Evert Duin for communicating unpublished results. We are grateful to Daniel Hartmann for the synthesis of the fluoro-analogue of HMBPP.

■ REFERENCES

(1) Eisenreich, W.; Bacher, A.; Arigoni, D.; Rohdich, F. *Cell. Mol. Life Sci.* **2004**, *61*, 1401.

(2) Wolff, M; Seemann, M.; Tse Sum Bui, B.; Frapart, Y.; Tritsch, D.; Garcia Estrabot, A.; Rodriguez-Concepcion, M.; Boronat, A.; Marquet, A.; Rohmer, M. *FEBS Lett.* **2003**, *541*, 115.

(3) Xiao, Y.; Chu, L.; Sanakis, Y.; Liu, P. *J. Am. Chem. Soc.* **2009**, *131*, 9931.

(4) Seemann, M.; Janthawornpong, K.; Schweizer, J.; Bottger, L. H.; Janoschka, A.; Ahrens-Botzong, A.; Tambou, E. N.; Rotthaus, O.; Trautwein, A. X.; Rohmer, M.; Schunemann, V. *J. Am. Chem. Soc.* **2009**, *131*, 13184.

(5) Grawert, T.; Span, I.; Eisenreich, W.; Rohdich, F.; Eppinger, J.; Bacher, A.; Groll, M. *Proc. Natl. Acad. Sci. U.S.A.* **2010**, *107*, 1077.

(6) Altincicek, B.; Duin, E. C.; Reichenberg, A.; Hedderich, R.; Kollas, A. K.; Hintz, M.; Wagner, S.; Wiesner, J.; Beck, E.; Jomaa, H. *FEBS Lett.* **2002**, *532*, 437.

(7) Rohdich, F.; Zepeck, F.; Adam, P.; Hecht, S.; Kaiser, J.; Laupitz, R.; Grawert, T.; Amslinger, S.; Eisenreich, W.; Bacher, A.; Arigoni, D. *Proc. Natl. Acad. Sci. U.S.A.* **2003**, *100*, 1586.

(8) Van Hoof, S.; Lacey, C. J.; Rohrich, R. C.; Wiesner, J.; Jomaa, H.; Van Calenbergh, S. *J. Org. Chem.* **2008**, *73*, 1365.

(9) Wang, W.; Wang, K.; Liu, Y.-L.; No, J. H.; Nilges, M. J.; Oldfield, E. *Proc. Natl. Acad. Sci. U.S.A.* **2010**, *107*, 4522.

(10) Wang, K.; Wang, W.; No, J. H.; Zhang, Y.; Zhang, Y.; Oldfield, E. *J. Am. Chem. Soc.* **2010**, *132*, 6719.

(11) Wang, W.; Li, J.; Wang, K.; Smirnova, T. I.; Oldfield, E. *J. Am. Chem. Soc.* **2011**, *133*, 6525.

(12) Ahrens-Botzong, A.; Janthawornpong, K.; Wolny, J. A.; Tambou, E. N.; Rohmer, M.; Krasutsky, S.; Poulter, C. D.; Schunemann, V.; Seemann, M. *Angew. Chem., Int. Ed.* **2011**, *50*, 11976.

(13) Xiao, Y.; Zhao, Z. K.; Liu, P. *J. Am. Chem. Soc.* **2008**, *130*, 2164.

(14) Grawert, T.; Rohdich, F.; Span, I.; Bacher, A.; Eisenreich, W.; Eppinger, J.; Groll, M. *Angew. Chem., Int. Ed.* **2009**, *48*, 5756.

(15) Rekittke, I.; Wiesner, J.; Rohrich, R.; Demmer, U.; Warkentin, E.; Xu, W.; Troschke, K.; Hintz, M.; No, J. H.; Duin, E. C.; Oldfield, E.; Jomaa, H.; Ermler, U. *J. Am. Chem. Soc.* **2008**, *130*, 17206.
(16) Xiao, Y.; Chang, W. C.; Liu, H. W.; Liu, P. *Org. Lett.* **2011**, *13*, 5912.
(17) Chang, W. C.; Xiao, Y.; Liu, H. W.; Liu, P. *Angew. Chem., Int. Ed.* **2011**, *50*, 12304.
(18) Citron, C. A.; Brock, N. L.; Rabe, P.; Dickschat, J. S. *Angew. Chem., Int. Ed.* **2012**, *51*, 4053.
(19) Lee, H. I.; Sorlie, M.; Christiansen, J.; Yang, T. C.; Shao, J.; Dean, D. R.; Hales, B. J.; Hoffman, B. M. *J. Am. Chem. Soc.* **2005**, *127*, 15880.
(20) Lee, H. I.; Igarashi, R. Y.; Laryukhin, M.; Doan, P. E.; Dos Santos, P. C.; Dean, D. R.; Seefeldt, L. C.; Hoffman, B. M. *J. Am. Chem. Soc.* **2004**, *126*, 9563.
(21) Kennedy, M. C.; Werst, M.; Telser, J.; Emptage, M. H.; Beinert, H.; Hoffman, B. M. *Proc. Natl. Acad. Sci. U.S.A.* **1987**, *84*, 8854.
(22) Werst, M. M.; Kennedy, M. C.; Beinert, H.; Hoffman, B. M. *Biochemistry* **1990**, *29*, 10526.
(23) Telser, J.; Emptage, M. H.; Merkle, H.; Kennedy, M. C.; Beinert, H.; Hoffman, B. M. *J. Biol. Chem.* **1986**, *261*, 4840.
(24) Span, I.; Grawert, T.; Bacher, A.; Eisenreich, W.; Groll, M. *J. Mol. Biol.* **2011**, *416*, 1.
(25) Belinskii, M. *Chem. Phys.* **1993**, *172*, 189.
(26) Mcmanus, H. J.; Fessenden, R. W.; Chipman, D. M. *J. Phys. Chem.* **1988**, *92*, 3778.
(27) Adedeji, D.; Hernandez, H.; Wiesner, J.; Kohler, U.; Jomaa, H.; Duin, E. C. *FEBS Lett.* **2007**, *581*, 279.
(28) Xu, W.; Lees, N. S.; Adedeji, D.; Wiesner, J.; Jomaa, H.; Hoffman, B. M.; Duin, E. C. *J. Am. Chem. Soc.* **2010**, *132*, 14509.
(29) Staples, C. R.; Ameyibor, E.; Fu, W.; Gardet-Salvi, L.; Stritt-Etter, A. L.; Schurmann, P.; Knaff, D. B.; Johnson, M. K. *Biochemistry* **1996**, *35*, 11425.
(30) Staples, C. R.; Gaymard, E.; Stritt-Etter, A. L.; Telser, J.; Hoffman, B. M.; Schurmann, P.; Knaff, D. B.; Johnson, M. K. *Biochemistry* **1998**, *37*, 4612.
(31) Walters, E. M.; Garcia-Serres, R.; Jameson, G. N.; Glauser, D. A.; Bourquin, F.; Manieri, W.; Schurmann, P.; Johnson, M. K.; Huynh, B. H. *J. Am. Chem. Soc.* **2005**, *127*, 9612.
(32) Wang, W.; Li, J.; Wang, K.; Huang, C.; Zhang, Y.; Oldfield, E. *Proc. Natl. Acad. Sci. U.S.A.* **2010**, *107*, 11189.
(33) Wang, W.; Wang, K.; Li, J.; Nellutla, S.; Smirnova, T. I.; Oldfield, E. *J. Am. Chem. Soc.* **2011**, *133*, 8400.
(34) Xu, W.; Lees, N. S.; Hall, D.; Welideniya, D.; Hoffman, B. M.; Duin, E. C. *Biochemistry* **2012**, *51*, 4835.
(35) Liu, Y. L.; Guerra, F.; Wang, K.; Wang, W.; Li, J.; Huang, C.; Zhu, W.; Houlihan, K.; Li, Z.; Zhang, Y.; Nair, S. K.; Oldfield, E. *Proc. Natl. Acad. Sci. U.S.A.* **2012**, *109*, 8558.
(36) Schmidt, T. G.; Skerra, A. *Nat. Protoc.* **2007**, *2*, 1528.
(37) Stoll, S.; Schweiger, A. *J. Magn. Reson.* **2006**, *178*, 42.
(38) Bernstein, F. C.; Koetzle, T. F.; Williams, G. J.; Meyer, E. F., Jr; Brice, M. D.; Rodgers, J. R.; Kennard, O.; Shimanouchi, T.; Tasumi, M. *Eur. J. Biochem.* **1977**, *80*, 319.
(39) Kabsch, W. *J. Appl. Crystallogr.* **1993**, *26*, 795.
(40) Brunger, A. T.; Adams, P. D.; Clore, G. M.; DeLano, W. L.; Gros, P.; Grosse-Kunstleve, R. W.; Jiang, J. S.; Kuszewski, J.; Nilges, M.; Pannu, N. S.; Read, R. J.; Rice, L. M.; Simonson, T.; Warren, G. L. *Acta Crystallogr., Sect. D* **1998**, *54*, 905.
(41) Emsley, P.; Cowtan, K. *Acta Crystallogr., Sect. D* **2004**, *60*, 2126.
(42) Murshudov, G. N.; Vagin, A. A.; Dodson, E. J. *Acta Crystallogr., Sect. D* **1997**, *53*, 240.
(43) Perrakis, A.; Harkiolaki, M.; Wilson, K. S.; Lamzin, V. S. *Acta Crystallogr., Sect. D* **2001**, *57*, 1445.
(44) *PyMOL*, v1.5.0.1; Schrödinger, LLC, 2012, http://www.pymol.org.
(45) Laskowski, R. A.; Rullmann, J. A.; MacArthur, M. W.; Kaptein, R.; Thornton, J. M. *J. Biomol. NMR* **1996**, *8*, 477.
(46) Hecht, S.; Amslinger, S.; Jauch, J.; Kis, K.; Trentinaglia, V.; Adam, P.; Eisenreich, W.; Bacher, A.; Rohdich, F. *Tetrahedron Lett.* **2002**, *43*, 8929.
(47) Fox, D. T.; Poulter, C. D. *J. Org. Chem.* **2002**, *67*, 5009.